A Metal-Chelating Microscopy Tip as a New Toolbox for Single-Molecule Experiments by Atomic Force Microscopy

Lutz Schmitt,*† Markus Ludwig,† Hermann E. Gaub,† and Robert Tampé*
*Institut für Physiologische Chemie, Philipps-Universität Marburg, 35033 Marburg, and †Lehrstuhl für Angewandte Physik, Ludwig-Maximilians Universität München, 80799 München, Germany

ABSTRACT In recent years, the atomic force microscope (AFM) has contributed much to our understanding of the molecular forces involved in various high-affinity receptor-ligand systems. However, a universal anchor system for such measurements is still required. This would open up new possibilities for the study of biological recognition processes and for the establishment of high-throughput screening applications. One such candidate is the *N*-nitrilo-triacetic acid (NTA)/His-tag system, which is widely used in molecular biology to isolate and purify histidine-tagged fusion proteins. Here the histidine tag acts as a high-affinity recognition site for the NTA chelator. Accordingly, we have investigated the possibility of using this approach in single-molecule force measurements. Using a histidine-peptide as a model system, we have determined the binding force for various metal ions. At a loading rate of 0.5 μm/s, the determined forces varied from 22 $\pm$ 4 to 58 $\pm$ 5 pN. Most importantly, no interaction was detected for Ca^{2+} and Mg^{2+} up to concentrations of 10 mM. Furthermore, EDTA and a metal ion reloading step demonstrated the reversibility of the approach. Here the molecular interactions were turned off (EDTA) and on (metal reloading) in a switch-like fashion. Our results show that the NTA/His-tag system will expand the "molecular toolboxes" with which receptor-ligand systems can be investigated at the single-molecule level.

INTRODUCTION

Over the last decade, the *N*-nitrilo-triacetic acid (NTA)/His-tag system has become a powerful and extremely popular tool in the biosciences for the one-step isolation and purification of gene products (Hochuli, 1990; Hochuli et al., 1988). The tetradental ligand NTA forms a hexagonal complex with divalent metal ions (Me^{2+}) such as Ni^{2+}, Co^{2+}, Cu^{2+}, or Zn^{2+} occupying four of the six binding sites in the complex. The remaining two binding sites are accessible to electron donor groups. In the case of proteins, these electron donor groups are the side chains of amino acids such as histidine, cysteine, and, to some extent, glutamate, aspartate, arginine, or lysine. As a prerequisite, these side chains have to be oriented in the right geometry to fit to the coordination sphere of the hexagonal Me^{2+}-NTA complex. The principle of attaching a protein to the complex by complex formation has been made generally applicable for protein purification by introducing a short stretch of five to six histidines at defined positions of the protein, creating a so-called histidine (His)-tagged fusion protein (Arnold, 1992). The His-tag has enough flexibility to bind to both unoccupied binding sides of the Me^{2+}-NTA complex synergistically. The two His/one NTA stoichiometry creates a stable immobilization so that the protein can be affinity purified. On the other hand, the stability of a one His/one NTA complex is too small for stable complex formation. In addition, two electron-donating amino acids on the surface of a protein with the appropriate orientation to form the required 2:1 stoichiometry is rarely encountered. Therefore, nonspecific binding of proteins without a His-tag is normally not observed. Finally, adsorbed proteins can easily be deimmobilized by the addition of EDTA or imidazole or by acidification.

A first attempt to utilize the concept of "metal chelating" proteins as a tool for biophysical studies was performed by Ill and co-workers (Ill et al., 1993). Here, a mica surface was doped with Ni^{2+} ions to immobilize a "metal-chelating peptide"-tagged antibody. Since the introduction of chelator lipids based on either the NTA headgroup (Schmitt et al., 1994) or iminodiacetic acid (IDA) (Shnek et al., 1994), these systems have been used in a wide variety of applications for the specific immobilization of His-tagged fusion proteins at surfaces. Examples include lipid monolayers (Dietrich et al., 1995, 1996; Schmitt et al., 1996), liposomes (Dorn et al., 1998), gold surfaces for applications in surface plasmon resonance spectroscopy (Sigal et al., 1996), and two-dimensional crystallization at lipid interfaces (Celia et al., 1999; Kubalek et al., 1994; Venien-Bryan et al., 1997; Wilson-Kubalek et al., 1998). In all of these examples, the highly specific binding process is used to immobilize the protein in an oriented and native conformation. Moreover, the reversible binding of His-tagged biomolecules to these metal-chelating molecules makes it possible to screen different biomolecules or to make a rather straightforward modification of the experimental conditions.

Although various studies have addressed the thermodynamic properties of the NTA chelator and related systems, nothing is known about the mechanical strength of the complex bond between the Me^{2+}-NTA complex and His-tagged biomolecules. One way to obtain this kind of information is to apply atomic force microscopy (AFM). AFM (Binnig and Rohrer, 1986) has been employed to determine the mechanical

Received for publication 16 July 1999 and in final form 9 March 2000.

Address reprint requests to Dr. Lutz Schmitt, Institut für Physiologische Chemie, Philipps-Universität Marburg, 35033 Marburg, Germany. Tel.: +49(6421)286-5046; Fax: +49(6421)286-4335; E-mail: schmittl@mailer.uni-marburg.de.

0006-3495/00/06/3275/11 $2.00

forces of, for example, the biotin-streptavidin system (Florin et al., 1994; Lee et al., 1994b), antibody-antigen systems (Dammer et al., 1995), and DNA strands (Lee et al., 1994a).

Here we have utilized the AFM to measure forces between the His-tag and the NTA complex loaded with various metal ions. To functionalize the AFM, gold-thiol chemistry was applied (Bain et al., 1989; Laibinis et al., 1989). A gold-coated AFM cantilever served as a surface for the immobilization of a NTA-thiol. To prevent steric hindrance in the recognition process, a triethylene-glycol-thiol was used as a matrix molecule. This approach creates a self-assembled monolayer (SAM) that coats the AFM tip. Because of the triethylene-glycol moiety, nonspecific adsorption is minimized, as shown by Whitesides and co-workers (Pale-Grosdemange et al., 1991). Furthermore, dilution of the NTA-thiol within the matrix thiol reduced the probability that a single His-tag binds to more than one NTA-thiol. As a model for His-tagged biomolecules, a polypeptide chain containing six histidines and a flexible, hydrophilic spacer was employed (Fig. 1) (Dietrich et al., 1995). This setup enabled us to study the complex formation between chelator and His-tag in detail with minimal interference from nonspecific steric or electrostatic interactions. In this investigation, rupture forces were investigated at a constant pulling rate of 0.5 μm/s. This setup does not determine the dependence of the measured force on the pulling rate. Such an influence has been shown experimentally for other systems (Evans and Ritchie, 1997; Merkel et al., 1999; Simson et al., 1999) and is expected for the NTA/His-tag system as well. However, the goal of the investigation was to verify whether the NTA/His-tag could be employed in principle in single-molecule experiments. Our data demonstrate that the metal ion incorporated into the NTA chelator has a profound influence on the kinetics of the forces of the NTA/His-tag system. Consequently, proper choice of the metal ion in combination with the surface modifications employed here will extend the "toolbox" available for AFM-based single-molecule measurements.

MATERIALS AND METHODS

Materials

Undec-10-enyl-bromide was purchased from Lancester (Mülheim, Germany). Triethylene-glycol and thioacetic acid were obtained from Aldrich (Steinheim, Germany). *N*ε-Z-L-Lysine was ordered from Bachem (Heidelberg, Germany). Thin-layer chromatography (TLC) plates (silica F_{254}) and silica gel 60 (mesh 230–400) were from Merck (Darmstadt, Germany). All other chemicals and solvents were purchased from Fluka (Neu-Ulm, Germany). Reactions were monitored by TLC and visualized by UV or stained with iodine, bromocresol green, ninhydrine, and potassium permanganate.

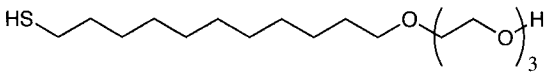

Triethylene-glycol-alkyl-thiol 5 (EO_3-thiol)

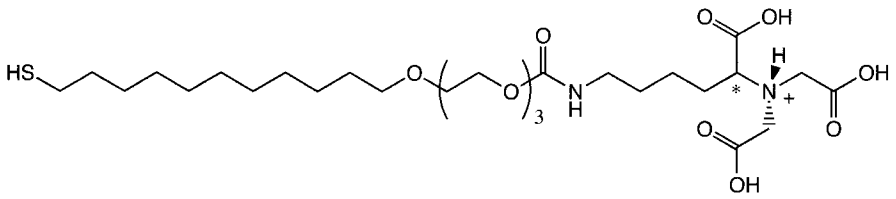

NTA-triethylene-glycol-alkyl-thiol 9 (NTA-thiol)

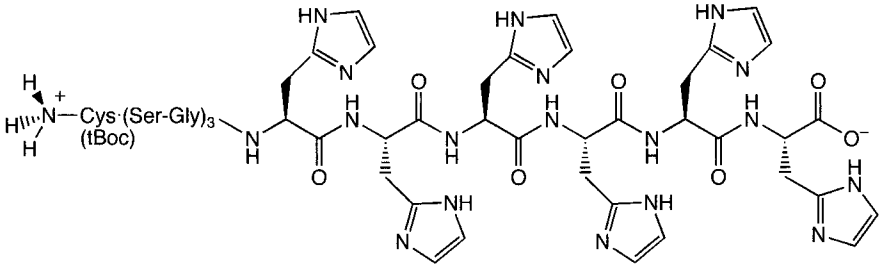

Cys(tBoc)-[(Gly-Ser)$_3$]-His-His-His-His-His-His (Histidine-peptide)

FIGURE 1 Molecules used in this study. The EO_3-thiol **5** was used as a matrix molecule to prevent steric hindrance between the NTA-thiol **9** and the immobilized histidine-peptide as well as nonspecific interaction with the modified tip. The histidine-peptide was synthesized and purified as described (Dietrich et al., 1995).

Solvent ratios are given as volume/volume. ^{1}H-NMR (500 or 400 MHz) was recorded on a Bruker AM 500 or 400 and ^{13}C-NMR (100 MHz) on a Bruker AM 400, using solvent as internal standards. Mass spectrometry (MS) (Finnigan; MAT, Foster City, CA) was performed in the negative and positive fast atomic bombardment (FAB) modes.

METHODS

Synthesis of NTA-thiol 9 and triethylene-glycol-thiol (EO_3-thiol) 5

The synthetic route is outlined in Fig. 2. Further details, including TLC, NMR, and MS data, can be found in the Supplementary Materials. The triethylene-glycol moiety was introduced by coupling the ω-unsaturated alkyl-bromide **1** to triethylene-glycol **2**. In the next step, the sulfur group was introduced by photochemical condensation of thioacetic acid to the terminal double bond, using high-power UV light and azo-bis-isobutyronitrile (AIBN). Removal of the sulfur protection group created the matrix molecule triethylene-glycol-thiol **5**. The NTA-thiol was synthesized by activating the intermediate **4** with carbonyl-diimidazole (CDI). The CDI adduct **6** is stable enough to be isolated by silica column chromatography and can be stored under nitrogen at −20°C. The imidazolid **6** reacted with the primary amino function of the NTA derivative **7** (Schmitt et al., 1994) at pH 10.3 in a water/dimethylformamide mixture. The formed carbamate **8** is stable under these conditions and can be extracted with ethyl acetate after the pH is adjusted to 1.5. Finally, the sulfur protection group is cleaved and the NTA-thiol isolated by a simple extraction step. Because of the acid lability of the carbamate moiety, the protection group has to be removed by triethylphosphine/oxygen.

Modification of carboxymethyl-dextran-coated gold surfaces

The histidine-peptide was covalently attached to carboxymethyl-dextran (molecular weight of the dextran, ~500,000 g/mol; Löfås, 1995)-coated gold chips (CM-5 chip) according to the protocol of the manufacturer (Biacore, Uppsala, Sweden). Briefly, the chips were activated by incubation in 0.2 M (1-ethyl-3-dimethylamino-propyl)carbodiimide (EDAC)/0.05 M sulfo-*N*-hydroxy succinimide (sulfo-NHS) for 5 min. This results in the activation of only 40% of the available carboxy functions. The histidine-peptide was then coupled by transferring the chips into a 1 mM histidine-peptide solution (10 mM NaOAc, pH 8.0). The reaction was stopped after 30 min, and unreacted NHS-esters were quenched by transferring the biofunctionalized chips into a 1 M ethanolamine solution (pH 8.0). After 30 min, chips were repeatedly rinsed with Millipore water and stored at 4°C until further use.

Modification of AFM tips

Commercially available AFM tips were gold-coated by vapor deposition of gold to yield a homogeneous 30–50-nm-thick gold layer. To prepare mixed SAMs, gold surfaces were incubated in 1 mM solutions of EO_3-thiol **5**/NTA-thiol **9** (9:1, mol%/mol%) in absolute ethanol for 12–20 h. Formation of the Ni-NTA complex was achieved by incubating the SAM for 5 min in 1 mM NaOH and for 60 min in 40 mM $NiSO_4$. Inhibition experiments were performed with 1 mM EDTA or 200 mM imidazole in phosphate-buffered saline (PBS) (pH 7.0).

AFM measurements

All measurements were performed on a home-built stylus-like instrument (Ludwig et al., 1997). Force scans (Fig. 3) were acquired at room temperature and analyzed according to the method of Florin et al. (1994). Scanning speed in all experiments was 0.5 μm/s (identical retract and approach speed), with a scanning amplitude of ~500 nm and minimal variation in the *x-y* plane. Three hundred to five hundred force scans were acquired to generate histograms (Figs. 4 and 5). These were used to determine the force necessary to disrupt the complex bond between the histidine-peptide and the NTA-thiol immobilized on the AFM tip. Because of the surface modifications employed, the numbers of the receptor (histidine-peptide) as well as the ligand (NTA-thiol) are diluted within the corresponding matrixes. Thus the actual recognition events between the metal chelator and the His-tag were reduced dramatically. In nearly all of the force scans analyzed, we observed either no (~20%) or only a single (~75%) rupture event, but only rarely two (<5%) and never more than two events.

Calibration of the cantilevers, smallest detectable force difference, and errors

Cantilevers were calibrated by measuring the thermal excitation (Florin et al., 1995). The spring constant of the cantilevers was ~60 pN/nm. In contrast to the free cantilever, binding of the cantilever to the surface through the specific ligand-receptor interaction reduces the thermal noise of the force signal as one approaches point *B* in Fig. 3. To further reduce the spikes in the measurements, a box-smoothing window (width 20 steps) was applied to the data shown (Rief et al., 1999a). In addition, only the averaged signal after point *B* to point *C* was used. Therefore, the smallest detectable force between the averaged free cantilever signal (Fig. 3, *B* and *C*) and the signal at point *B* was 10 pN. However, all forces below 15 pN were omitted from the recorded data and are not shown in the histograms (Figs. 4 and 5). The errors given in Table 1 are the standard deviations of multiple experiments (up to five) for each metal ion for different cantilevers and samples.

RESULTS

To determine the molecular forces between a metal chelator and a histidine-peptide as a simple model for His-tagged proteins, we employed a modified AFM setup. The molecules used in this study are shown in Fig. 1. The histidine-peptide was immobilized on a carboxymethyl-dextran layer coupled to a gold surface by standard active ester chemistry. This technique is now widely used to immobilize proteins and other biomolecules (for example, in the Biacore setup; Biacore, Uppsala, Sweden; Löfås and Johnson, 1990). To utilize the AFM in a straightforward manner, gold-thiol chemistry was applied to modify the AFM tip. A 30–50-nm-thick gold layer was evaporated onto the tip surface. The layer of gold was used to create a SAM of the NTA-thiol **9** (Fig. 1) on the tip. To prevent steric or electrostatic interactions between individual NTA complexes, the SAM consisted of two species. As a matrix molecule, the EO_3-thiol **5** (Fig. 1) was added to yield a 1:9 (mol%/mol%) mixture of NTA-thiol **9**:EO_3-thiol **5**. The histidine-peptide was synthesized by solid-phase peptide synthesis as described (Dietrich et al., 1995). The synthesis of the thiols **5** and **9** is summarized in Fig. 2. It follows the procedures developed by Whitesides and co-workers (Pale-Grosdemange et al., 1991; Sigal et al., 1996) with some modifications, which enabled us to synthesize both thiols following

the same strategy. A brief description of the synthesis is given in Materials and Methods. Further details, including TLC, NMR, and MS data, are given in the Supplementary Materials.

The molecules shown in Fig. 1 in combination with the described modified AFM setup were used to determine the molecular force of the complex bond between the histidine-peptide and the NTA complex. Force scans such as the one shown schematically in Fig. 3 are the basis for this determination. Here changes in the physical interaction between the modified AFM tip (NTA-thiol) and the dextran surface (histidine-peptide) result in changes in the bending of the AFM tip, which are used to extract the molecular force. Three stages can be distinguished during the retracting phase. Up to position A, the functionalized AFM tip has penetrated the dextran layer and is on top of the gold surface. The exact location of position A in the individual force scans was determined as described (Ludwig et al., 1997). Increasing the distance between tip and surface resulted in large changes in the corresponding force. Removing the cantilever from the surface abolishes the nonspecific repulsive force. Between positions A and B the dextran polymer between tip and surface is stretched more and more (Rief et al., 1997b). Finally, at position B the applied force is equal to the molecular force at this particular pulling rate between the NTA complex (attached to the AFM tip by

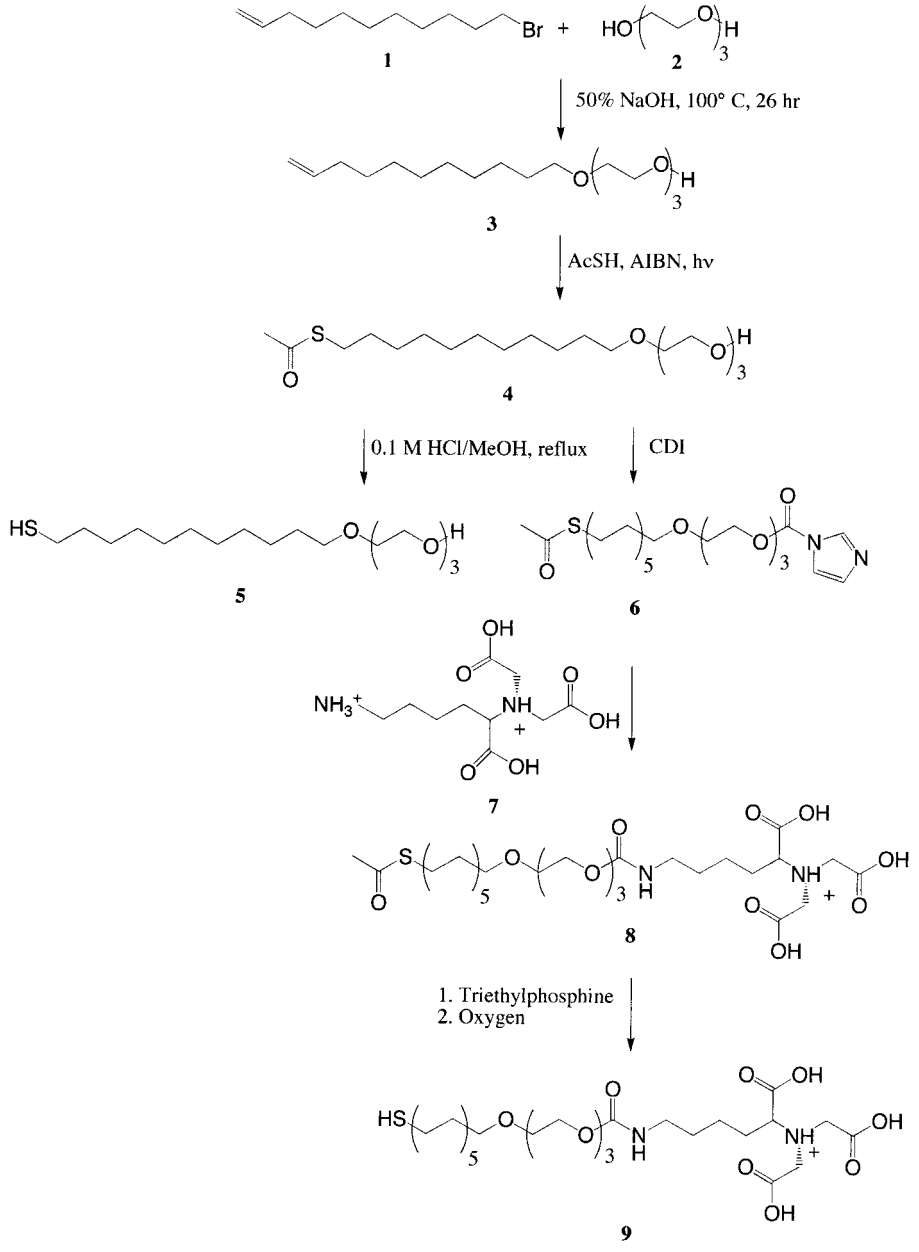

FIGURE 2 Summary of the synthetic route of the matrix EO_3-thiol **5** and the NTA-thiol **9**. Details of the synthesis are given in Materials and Methods.

gold-thiol chemistry) and the histidine-peptide (covalently immobilized to the dextran layer). A slight increase in the force results in the rupture of the complex bond. Now the cantilever is again in the relaxed (noninteracting) state C. The change in bending force between B and C is therefore equal to the force between the two interacting molecules at a constant loading rate. After bond cleavage (B-C), the two species (NTA-complex and His-tag) no longer interact with each other. Thus the signal obtained is a straight line (position C). This procedure is repeated for a defined number of experiments and added together, yielding a histogram. Here the frequency of events versus force is plotted. The exact experimental details and receptor densities will dictate the number of events. In our case, both the NTA-thiol **9** and the histidine-peptide were attached to the corresponding surfaces in a very diluted manner. For the NTA-thiol **9**, dilution was achieved by simply mixing the thiol with the matrix thiol **5** in a 1:9 ratio. The ratio of the two thiols in solution and on the surface is identical within the experimental error (Sigal et al., 1996). The histidine-peptide was covalently coupled to carboxy functions on the modified dextran layer. Here not more than 40% of the potential binding sites on the polymer can be derivatized with the ligand (Löfás and Johnson, 1990; Löfás, 1995). Consequently, we rarely observed more than one event (<5%). In most of the force scans only one bond rupture was detectable (~ 75%), while no events were measured in ~20% of all scans.

Using the described setup (Fig. 3), the molecular forces between the histidine-peptide and the NTA complex were analyzed as a function of various divalent cations. Preparation of the SAMs and the loading of the empty NTA complex with the employed metal ions are described in

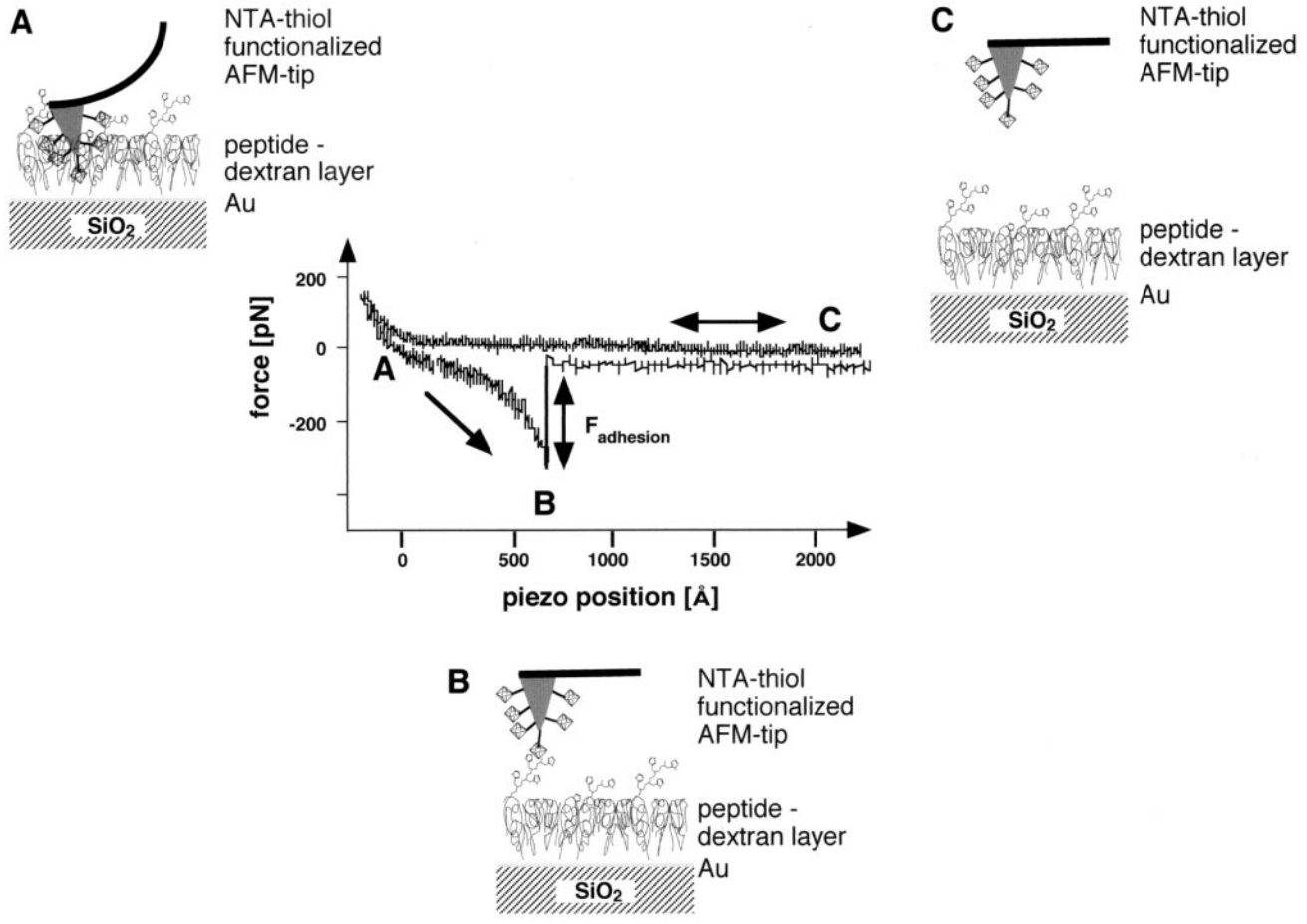

FIGURE 3 AFM force scan. The principal events are discussed for the situation after the tip approaches the surface until it is in contact and bend upward. (*A*) Movement of the AFM tip from the surface reduces nonspecific interactions with the gold surface and the dextran layer. (*B*) The bond between the functionalized NTA tip and immobilized histidine-peptide yields the actual binding force of the complex-ligand system under the influence of the applied force. At the moment when the complex bond ruptures, a large change in the cantilever signal is detected. This change is equal to the adhesive force between the two partners. The distance between *A* and *B* is ~50–100 nm. (*C*) After the rupture of the NTA complex and the immobilized histidine-peptide, there is no longer a physical interaction between the two molecules. As a result no changes in the cantilever position occur. Consequently, a constant signal is detected (equal to a constant force). Raw data like that shown here were analyzed as described in Materials and Methods.

Materials and Methods. Histograms summarizing our experiments are given in Fig. 4. In addition to the four metal ions shown (*A*: Co^{2+}; *B*: Cu^{2+}; *C*: Ni^{2+}; *D*: Zn^{2+}), Ca^{2+} and Mg^{2+} were investigated (data not shown). For the latter two ions, no interaction was observed. Additional experiments in the absence of metal ions, NTA-thiol, or the histidine-peptide were performed (data not shown). In all of these cases, no interactions were observed. Therefore, the

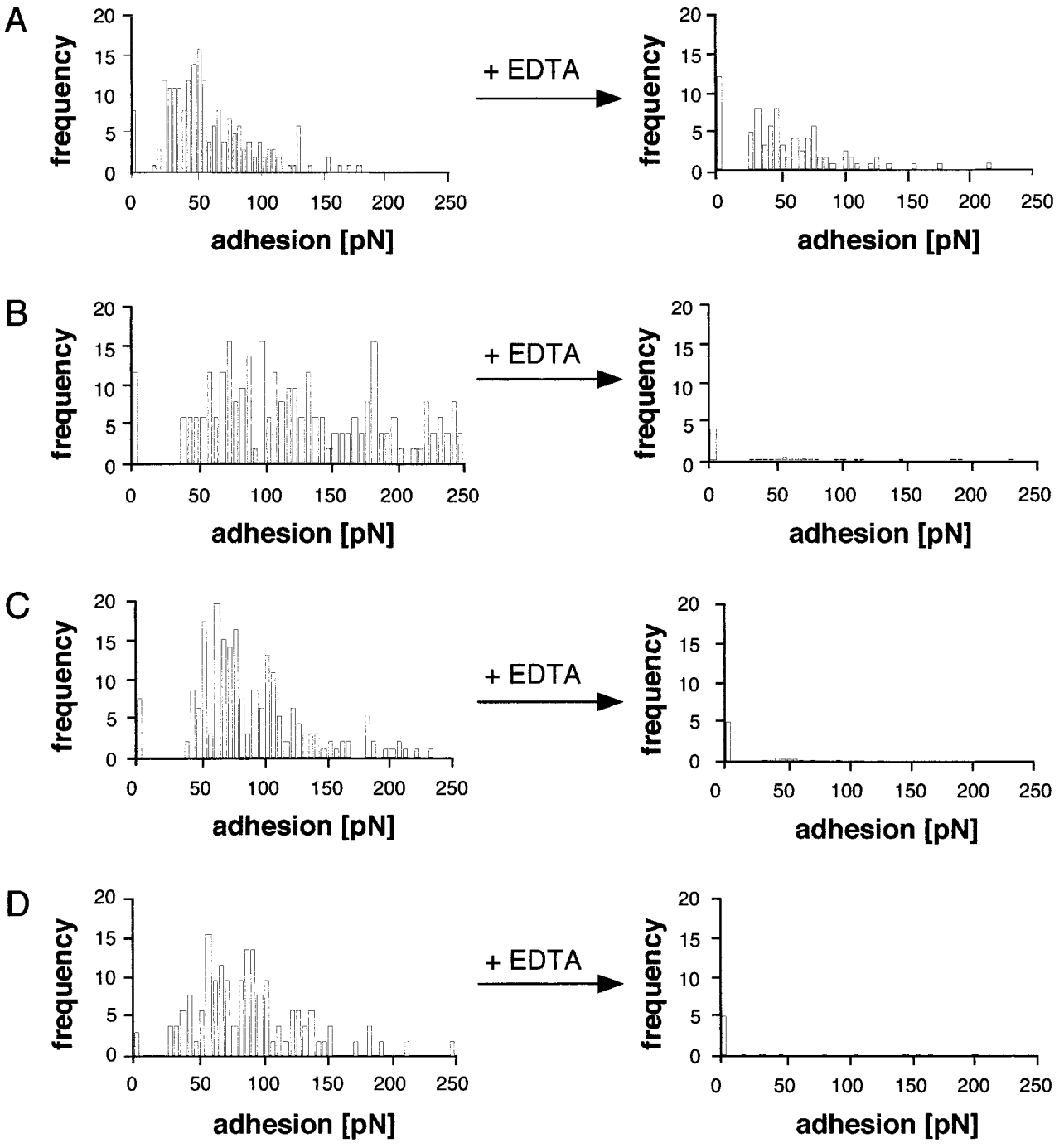

FIGURE 4 Histograms of force scans at a constant loading rate of 0.5 μm/s between the dextran-immobilized histidine-peptide and the NTA complex for various divalent metal ions. (*A*) Co^{2+}; (*B*) Cu^{2+}; (*C*) Ni^{2+}; (*D*) Zn^{2+}. (*Left*) Histograms for the Me^{2+}-NTA/histidine-peptide interactions. (*Right*) Histograms for the same systems are given after incubation of the metal-chelating AFM tip for 30 min in a 1 mM EDTA solution. For the experiments after EDTA treatment, between 300 and 500 scans were recorded, but only the events shown resulted in a detectable force.

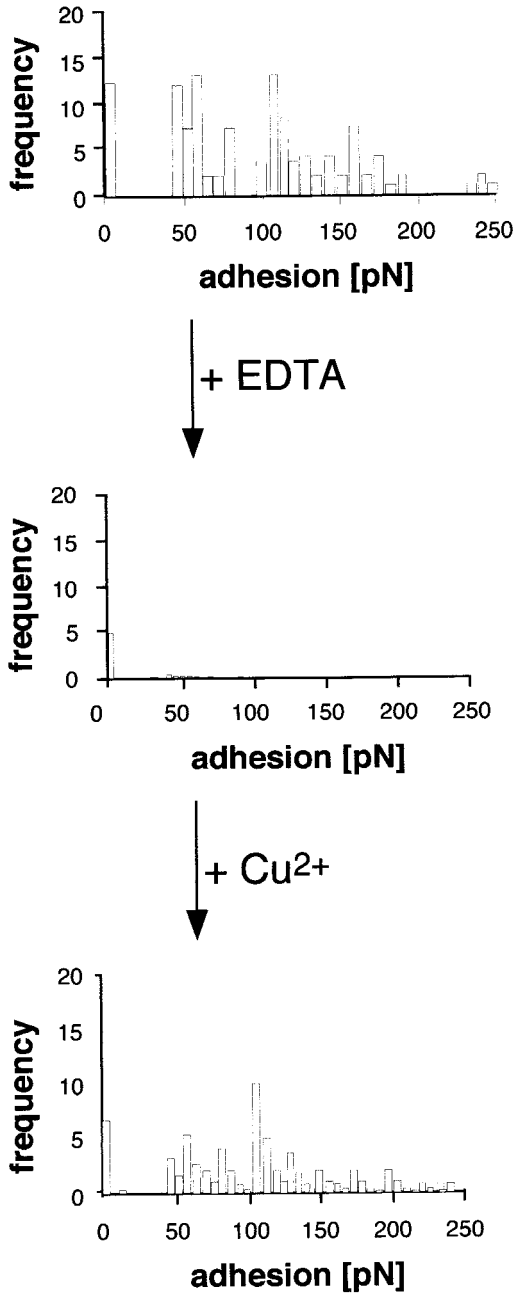

FIGURE 5 Histograms for the Cu^{2+}-NTA/histidine-peptide systems, demonstrating the proposed reversibility of the NTA/His-tag system. (*A*) Histogram for the loaded Cu^{2+}-NTA/histidine-peptide system. (*B*) Histogram after incubation of the NTA-functionalized AFM tip in 1 mM EDTA, pH 7.0 solution. Between 300 and 500 scans were recorded, but only the events shown in the right panel resulted in a detectable force. (*C*) Histogram after reloading of the NTA group with Cu^{2+} as described in Materials and Methods.

histograms shown in Fig. 4 (*left*) represent the metal-ion-dependent molecular forces between the loaded Me^{2+}-NTA complex and the histidine-peptide. For every metal ion distinct events and rupture of more than one NTA/His-tag complex are visible. The binding forces of the interaction between the metal-loaded NTA complex and the histidine-peptide were analyzed according to the procedures described by Florin et al. (1994) and were summarized in Table 1. The observed forces are a factor of 3–5 smaller than the one observed for the biotin-streptavidin system (Moy et al., 1994).

One of the major advantages of the NTA/His-tag system is the gentle way in which immobilized His-tag proteins can be deimmobilized. To achieve this goal, the addition of competitors such as imidazole, acidification, and the addition of EDTA are commonly employed. To investigate the reversibility of binding, NTA-thiol-modified AFM tips loaded with various metal ions were incubated in a 1 mM EDTA solution for 30 min (Fig. 4, *right*). (For further details see Materials and Methods.) As shown, no interaction between the AFM tips incubated for 30 min in a EDTA solution and the dextran-immobilized histidine-peptide was observed for Cu^{2+}, Ni^{2+}, and Zn^{2+} (Fig. 4, *B–D, right*). A drastically reduced but still measurable interaction was observed for the Co^{2+}-NTA system (Fig. 4 *A, right*). While the frequency of interaction was reduced by a factor of 3, the characteristic pattern and maxima for the molecular forces of the interaction seen for the Co^{2+}-loaded NTA complex were still detectable after incubation of the AFM tip in an EDTA solution. Only after prolonged incubations ($>$180 min), an interaction was completely abolished.

A prerequisite for the use of the NTA/His-tag system as an anchor in the force determination of various receptor-ligand systems is the ability to switch the interaction between the two molecules on and off in a defined fashion. To investigate this possibility, the experiment shown in Fig. 5 was performed. After loading of the NTA-thiol with Cu^{2+}, the histograms in Fig. 5 *A* were acquired. Incubation of the AFM tip in an EDTA solution resulted in a complete loss of detectable forces between the NTA complex and the immobilized histidine-peptide (Fig. 5 *B*). This interaction was regained by a subsequent incubation step of the NTA-thiol in a Cu^{2+} solution for 30 min (Fig. 5 *C*). A similar pattern of rupture events was observed again. Therefore, the Cu^{2+}-NTA complex was successfully reformed, displaying a similar interaction pattern in the second cycle.

TABLE 1 Molecular forces of the complex bond of the Me^{2+}-NTA/His-tag complex for various metal ions at a constant loading rate of 0.5 μm/s

Metal ion	Binding force (pN)
Co^{2+}	22 ± 4
Cu^{2+}	58 ± 5
Ni^{2+}	38 ± 4
Zn^{2+}	28 ± 3

Forces were extracted from the histograms given in Fig. 4. Errors given represent the standard deviation of at least five independent experiments.

DISCUSSION

Recently, a number of single-molecule experiments have been published that used the AFM (Dammer et al., 1995; Florin et al., 1994; Lee et al., 1994a,b; Rief et al., 1997a,b, 1998, 1999b). To further expand the possibilities of studying single molecules and their interaction by AFM, a system of general application is still needed. Such a system should guarantee uniform orientation of the molecule(s) under investigation. Furthermore, few or no nonspecific interactions and the ability to preserve the native state of the biomolecule are desired. One potential system is the NTA/His-tag system (Hochuli et al., 1988). This strategy is now generally used for the one-step isolation and purification of His-tagged fusion proteins. Consequently, a vast variety of such biomolecules are available. The immobilization process normally occurs under physiological conditions in a relatively specific manner. It is important to note that cations such as Ca^{2+} and Mg^{2+} do not influence the ability of the His-tag to bind to the NTA complex. Because of these advantages, the NTA/His-tag system has been used to immobilize fusion proteins at different interfaces, such as lipid monolayer (Dietrich et al., 1995, 1996; Schmitt et al., 1996; Shnek et al., 1994), vesicles (Dorn et al., 1998), or dextrane surfaces (Sigal et al., 1996), or to study the structure and function of macromolecular enzyme complexes (Dorn et al., 1999). Taken together, the NTA/His-tag system seems to be well suited to use as a general anchor system for single-molecule experiments. However, nothing is known about the forces needed to rupture the NTA/His-tag bond and the influence of the metal ion on the kinetics of bond rupture.

The molecules used to determine the molecular force and the synthesis of the NTA-thiol **9**, the matrix thiol, EO_3-thiol **5**, and the histidine-peptide are shown in Fig. 1. Thiol **5** reduces nonspecific interaction and adsorption of biomolecules (Pale-Grosdemange et al., 1991). Its presence diluted the NTA complexes, so that an undisturbed interaction of the histidine-peptide with the NTA complexes can be ensured. The flexibility of the triethylene glycol spacer guarantees that no steric constraints are put on the system. Furthermore, it was shown that the ratio of thiols **5** and **9** in solution corresponds to the ratio within the SAM (Sigal et al., 1996). Detailed studies performed with thioalkanes containing oligoethylene glycol headgroups of various lengths have established that these systems form monolayers at the gold surface (Pale-Grosdemange et al., 1991). The fact that the NTA headgroup is attached to the terminal hydroxy group of the triethylene glycol moiety and is highly diluted in the matrix thiol strongly suggests that this system behaves identically to other well-characterized thiols adsorbed to a gold surface (Bain et al., 1989; Pale-Grosdemange et al., 1991; Prime and Whitesides, 1993; Sigal et al., 1996). The employed coupling chemistry attaches the histidine-peptide in a defined way, with the His-tag always at the opposite end of the amide bond formed between the peptide and dextrane cushion. Nevertheless, a conformational fixation of the peptide does not take place. The flexibility and the physical properties of the dextrane cushion will generate a wide range of environments and orientations of the peptide. On the other hand, it has been shown that this cushion does not interfere with the applied forces and loading rate of our experiment (Rief et al., 1997b). As shown in Fig. 3, the modified AFM tip (receptor) will contact the peptide (ligand) in every possible orientation, thereby creating a continuum of molecular interactions and orientations. With removal of the tip, the molecular spring will align the receptor-ligand complexes and orient them uniformly. Thus, in the moment of bond rupture, the continuum of possible orientations will be reduced drastically.

Using the force scan technique and the molecules described, we analyzed various metal ions incorporated into the NTA complex and the binding force in these complexes at a constant loading rate (Fig. 4, *left*, and Table 1). In accordance with other studies (Schmitt et al., 1994), no interaction could be detected for Ca^{2+} and Mg^{2+} up to a concentration of 10 mM in the incubation step (data not shown). This finding is important for the application of this system as a general anchor system in biophysical studies. A lot of proteins require either Ca^{2+} or Mg^{2+} for their function and/or stability. This result demonstrates that neither ion interferes with the binding and recognition process. Force scans for Co^{2+}, Cu^{2+}, Ni^{2+}, and Zn^{2+} are given in Fig. 4 (*left*). The extracted binding forces are given in Table 1 and range from 22 ± 4 pN for Co^{2+} (Fig. 4 *A*) to 58 ± 5 pN for Cu^{2+} (Fig. 4 *B*). Comparing the stability of the various NTA complexes by means of the dissociation constant of the complex reveals that the Cu^{2+}-NTA complex has the highest thermodynamic stability in terms of the metal-NTA dissociation constant (Arnold, 1992). On the other hand, the metal ion mainly used in the purification of His-tag proteins (Ni^{2+}) displayed the highest frequency of events. This emphasizes again that some recognition processes can be kinetically controlled and the underlying thermodynamic parameters do not necessarily dictate the process.

The specificity of unbinding was shown by the addition of imidazole (data not shown) or EDTA (Fig. 4, *right*). For all metal ions except Co^{2+}, no interaction was detectable after incubation with EDTA for 30 min. In the case of Co^{2+} (Fig. 4 *A*, *right*), the observed interaction was drastically reduced but was still present. Prolonged incubation with EDTA resulted in a complete loss of detectable interaction (data not shown). This implies that the competition of EDTA and NTA for Co^{2+} is a kinetically hindered process.

One of the advantages of the NTA system is its reversibility. As has been shown for other surfaces (Gritsch et al., 1995; Sigal et al., 1996), Me^{2+}-NTA complexes can be reloaded by a subsequent incubation step. Such a switching on was also observed in our force scans (Fig. 5). Incubation of the NTA-modified cantilever with Cu^{2+} resulted in the

histogram shown in Fig. 5 *A*. Incubation of the tip in 1 mM EDTA for 30 min resulted in a complete loss of the Cu^{2+} complex through complex formation of the more stable Cu^{2+}-EDTA complex (Fig. 5 *B*). The interaction between the histidine-peptide and the NTA complex could be switched on by reloading the NTA complex with Cu^{2+} (Fig. 5 *C*). While the same periodicity of events was observed, differences in the frequency of events are visible. One possible explanation is that not all EDTA has been removed during the rinsing steps. If some EDTA remains physisorbed, it is possible that NTA and EDTA compete for the added Cu^{2+}. Consequently, a different loading pattern is to be expected. Nevertheless, the data indicate that NTA complexes can be reloaded and therefore reused. This opens up the possibility of scanning different receptors or ligands with the same modified AFM tip.

In recent years it has been demonstrated that forces encountered in biological systems depend strongly on the loading rate of the experimental conditions (Evans and Ritchie, 1997; Merkel et al., 1999). Thus the dissociation of a bond under a constant force represents only one point in a more or less continuous spectrum of strengths. With a varying loading rate (rate of applied force), the measured force of dissociation varies over at least two orders of magnitude for the biotin/streptavidin system (Merkel et al., 1999). An identical behavior is to be expected for the Me^{2+}-NTA/His-tag system. Here we have analyzed the force involved in the Me^{2+}-NTA/His-tag recognition at only one loading rate (0.5 μm/s). This value was chosen to compare our results directly with the force studies of the dextran (Rief et al., 1997b) and biotin/streptavidin (Florin et al., 1994; Moy et al., 1994). However, even at a constant loading rate, the strength of the NTA/His-tag varies by a factor of 2.5, depending on the metal cation incorporated in the NTA complex. Therefore, in addition to the expected dependence of the measured force on the applied loading rate, the NTA/His-tag system can be fine-tuned by the proper choice of metal ion. In cases where a high frequency of immobilization events is desirable, Ni^{2+} should be employed. In systems where a high rupture force is necessary, Cu^{2+} would be the metal ion of choice. Further analysis of various metal complexes might reveal metal ions with an even higher kinetic stability than Cu^{2+}-NTA.

The data presented here indicate that the Me^{2+}-NTA/His-tag approach can be used in principle to investigate the molecular forces of His-tagged biomolecules and their ligands by AFM. A vast variety of proteins can be functionally and uniformly immobilized onto NTA modified surfaces, because the principle of fusion proteins is an established procedure in all branches of bioscience. Probably equally important is the possibility of employing the herein described combination of AFM and the Me^{2+}-NTA/His-tag approach in screening assays. In summary, the application of the NTA/His-tag system will extend the "molecular toolbox" with which AFM experiments can be performed.

SUPPLEMENTARY MATERIALS

Synthesis of undec-10-enyl-triethylene-glycol 3

Fourteen grams (93 mmol) of triethylene-glycol **2** was dissolved in 1.5 ml (19 mmol) 50% NaOH and stirred for 2 h at 100°C under an atmosphere of nitrogen. After the addition of 4.4 g (18.8 mmol) undec-10-enyl-bromide **1** the mixture was stirred for 24 h at 100°C under an atmosphere of nitrogen. The reaction mixture was extracted six times with hexane. The combined organic phases were dried over anhydrous sodium sulfate, and solvent was removed in vacuum. The product was purified by silica column chromatography with ethyl acetate as the eluent.

Yield: 2.6 g (8.6 mmol) 46%.

R_f = 0.6 in ethyl acetate.

^{1}H-NMR (500 MHz, $CDCl_3$): δ = 1.25 (m, 14 H, CH_2), δ = 1.6 (m, 4 H, CH_2), δ = 2.2 (br s, 1 H, OH), δ = 3.4 (t, 2 H, OCH_2), δ = 3.75- 3.5 (m, 14 H, OCH_2CH_2), δ = 5.0 (m, 2 H, CH_2 = CH), δ = 5.3 (m, 1 H, CH_2═CH)

^{13}C-NMR (100 MHz, $CDCl_3$): δ = 139.9 (CH_2═CH), δ = 114.7 (CH_2═CH), δ = 73.2, 72.3, 71.46, 71. 1, 70.8, 62.5 (OCH_2CH_2), δ = 34.5, 30.3, 30.2, 30.1, 29.8, 29.6, 26.8 (CH_2)

MS (FAB pos., $C_{17}H_{34}O_4$): M + H^+ = 303.4 g/mol.

Synthesis of [1-[(methylcarbonylthio)undecyl-11] triethylene-glycol 4

Two milliliters (26 mmol) of thioacetic acid and 34 mg AIBN were added to a solution of 2.6 g (8.6 mmol) undec-11-enyl-triethylene-glycol **3** in 26 ml methanol. The solution was irradiated for 4 h under an atmosphere of nitrogen with a 250-W, high-pressure Hg lamp, filtered through Pyrex. Completeness of the photoreaction was monitored by the Bayer assay for unsaturated carbon bounds (1 mM potassium permanganate). Solvent was removed in vacuum, and the product was purified by silica column chromatography with ethyl acetate as the eluent.

Yield: 2.35 g (6.5 mmol) 76%.

R_f: 0.67 in ethyl acetate.

^{1}H-NMR (400 MHz, $CDCl_3$): δ = 1.25 (m, 14 H, CH_2), δ = 1.6 (m, 4 H, CH_2), δ = 2.3 (s, 3 H, CH_3), δ = 2.85 (t, 2 H, SCH_2), δ = 3.45 (t, 2 H, OCH_2), δ = 3.5 - 3.75 (m, 12 H, OCH_2CH_2).

^{13}C-NMR (100 MHz, $CDCl_3$): δ = 197.2 (C═O), δ = 73.2, 72.2, 71.3, 71.1, 70.7, 62.4 (OCH_2CH_2), δ = 31.2, 30.2, 30.1, 29.8, 29.7, 29.5, 26.7 (CH_2, CH_3).

MS (FAB pos., $C_{19}H_{38}O_5S$): M+H^+ = 379.3 g/mol.

Synthesis of (1-mercaptoundecyl-11)triethylene-glycol 5

[1-[(Methylcarbonylthio)undecyl-11]triethylene-glycol 4 (2.35 g, 6.5 mmol) was dissolved in 20 ml 0.1 N HCl in methanol and refluxed under an atmosphere of nitrogen for 4 h. Solvent was removed in a vacuum, and the product was purified by silica column chromatography with ethyl acetate/methanol (25:1) as the eluent.

Yield: 1.8 g (5.6 mmol) 87%.

R_f: 0.67 in ethyl acetate/methanol (25:1).

^{1}H-NMR (400 MHz, $CDCl_3$): δ = 1.2 (m, 15 H, CH_2), δ = 1.6 (m, 4 H, CH_2), δ = 2.2 (br s, 1 H, SH), δ = 2.5 (quar., 2 H, CH_2SH), δ = 3.4 (t, 2 H, CH_2OH), δ = 3.5–3.75 (m, 12 H, OCH_2CH_2).

^{13}C-NMR (100 MHz, $CDCl_3$): δ = 73.2, 72.3, 71.3, 71.1, 70.4, 62.5 (CH_2CH_2O), δ = 34.7, 30.2, 29.7, 29.1, 26.8, 25.3 (CH_2).

MS (FAB pos., $C_{17}H_{36}O_4S$): $M+H^+$ = 337.2 g/mol.

Synthesis of [11-[(methylcarbonylthio)undecyl-1] triethylene-glycol-carbonyl-imidazolid 6

[1-[(Methyl-carbonylthio)undecyl-11]triethylene-glycol **4** (430 mg, 1.14 mmol) was dissolved in 4 ml methylene chloride and stirred for 2 h at room temperature after the addition of 370 mg (2.3 mmol) carbonyldiimidazolide. Solvent was removed in vacuum, and the product was purified by silica column chromatography with ethyl acetate as the eluant.

Yield: 417 mg (0.9 mmol) 78%.

R_f: 0.46 in ethyl acetate.

^{1}H-NMR (400 MHz, CD_3OD): δ = 7.6 (d, 1 H, imidazol-H′-5), δ = 7.0 (d, 1 H, imidazol-H′-4), δ = 4.3 (t, 2 H, $CH_2OC(O)NH$), δ = 3.7–3.5 (m, 12 H, OCH_2CH_2), δ = 3.45 (t, 2 H, OCH_2), δ = 2.8 (t, 2 H, SCH_2), δ = 2.3 (s, 3 H, CH_3), δ = 1.6 (m, 4 H, CH_2), δ = 1.4–1.2 (m, 12 H, CH_2).

^{13}C-NMR (100 MHz, CD_3OD): δ = 197.6 ($CH_3C{=}OS$), δ = 138.8 (OC(O)NH), δ = 136.3 (imidazol-C-2), δ = 130.6 (imidazol-C-4), δ = 118.9 (imidazol-C-5), δ = 73.7, 72.4, 71.6, 71.1, 70.0, 69.6, 68.6, 68.1, 62.2 (CH_2CH_2O), δ = 40.1, 30.7, 30.6, 30.5, 30.1, 29.8, 29.7, 27.2 (CH_2, CH_3).

MS (FAB pos., $C_{23}H_{40}O_6N_2S$): $M+H^+$ = 473.3 g/mol.

Synthesis of N_α-[11-[(methylcarbonylthio)undecyl-1]triethylene-glycol-carbonyl]-N_α,N_α-methylcarboxyl-L-lysine 8

N_α,N_α-Methylcarboxy-L-lysine 7 (618 mg, 3.4 mmol), synthesized according to the method of Schmitt et al. (1994), was dissolved in 10 ml water, and the pH was adjusted to 10.3 with 50% NaOH. After the addition of 400 mg (0.85 mmol) [11-[(methylcarbonylthio)undecyl-1]triethylene-glycol-carbonyl-imidazolide in 10 ml dimethylformamide, the mixture was stirred at room temperature overnight. The reaction was quenched by the addition of 45 ml of water. The aqueous phase was extracted three times with ethyl acetate, and the organic phase was discarded. After the pH was adjusted to 1.5, the aqueous phase was extracted four times with ethyl acetate. The combined organic phases were washed once with saturated sodium chloride and dried over anhydrous sodium sulfate, and the solvent was removed in a vacuum.

Yield: 505 mg (0.76 mmol) 90%.

^{1}H-NMR (400 MHz, CD_3OD): δ = 1.3–1.9 (m, 24 H, CH_2), δ = 2.2 (t, 2 H, $NHCH_2$), δ = 2.3 (s, 3 H, CH_3), 2.8 (t, 2 H, SCH_2), δ = 3.1 (t, 1 H, CH), δ = 3.3–3.7 (m, 18 H).

^{13}C-NMR (100 MHz, CD_3OD): δ = 196.1 ($CH_3C(O)S$), δ = 175.9, 175.1 (COO^-), δ = 158. 9 (OC(O)NH), δ = 77.9 (CH_2COO^-), δ = 72.4, 71.6, 71.1, 67.3, 66.7, 66.4 (CH_2CH_2O), δ = 55.4 (CH), δ = 41.51, 35.0, 30.7, 30.5, 30.1, 29.5, 28.7, 25.9, 24.6, 19.6, 14.41 (CH_2, CH_3).

MS (FAB pos., $C_{30}H_{54}N_2O_{12}S$): $M+H^+$ = 667.4 g/mol.

Synthesis of N_α-[11-mercapto-undecyl-1] triethylene-glycol-carbonyl]-N_α,N_α-methylcarboxyl-L-lysine 9

N_α-[11-[(Methylcarbonyl-thio)undecyl-1]triethylene-glycol-carbonyl]-N_α,N_α-methyl-carboxyl-L-lysine **8** (500 mg, 0.76 mmol) was dissolved in 2.5 ml dimethoxy-ethane, 2.2 ml water, and 0.8 ml 1 N NaOH. After the addition of 2.5 mg iodine, oxygen was bubbled through the reaction mixture for 4 h. The reaction was quenched by the addition of 13 ml water. After the pH was adjusted to 1.5, the precipitated disulfide was filtered off and dried in vacuum. The disulfide was dissolved in 11 ml methanol and 4 ml water under an atmosphere of nitrogen. After the addition of 2.4 ml (2.4 mmol) 1 M triethylphosphine in THF, the solution was stirred at room temperature under an atmosphere of nitrogen for 4 h. The reaction was quenched by the addition of 12 ml degassed water and the pH adjusted to 1.5. The aqueous phase was extracted three times with 25 ml ethyl acetate. The combined organic phases were washed once with saturated sodium chloride and dried over anhydrous sodium sulfate, and the solvent was removed in vacuum.

Yield: 113 mg (0.16 mmol) 40%.

^{1}H-NMR (400 MHz, CD_3OD): δ = 4.3–4.0 (m, 19 H), δ = 3.1 (quart., 2 H), δ = 2.0 (quart., 2 H), δ = 1.7- 1.2 (m, 23 H).

MS (FAB pos., $C_{37}H_{52}N_2O_{11}S$): $M+H^+$ = 625 g/mol.

We thank I. Dorn, M. Rief, and W. Dettmann for many stimulating discussions; U. Rädler for critical reading of the manuscript; and I. Zettl and Dr. H. Schäfer for NMR and MS measurements. Special thanks to R. Merkel for stimulating discussion and critical reading of the manuscript.

Financial support came from the Deutsche Forschungsgemeinschaft and the Volkswagen-Stiftung (HEG and RT) as well as the European Commission Biotechnology program (RT).

REFERENCES

Arnold, F. H. 1992. Metal Affinity Protein Separations. Academic Press, San Diego.

Bain, C. D., E. B. Troughton, Y.-T. Tao, J. Evall, G. M. Whitesides, and R. G. Nuzzo. 1989. Formation of monolayer films by the spontaneous assembly of organic thiols from solution onto gold. *J. Am. Chem. Soc.* 111:321–335.

Binnig, G., and H. Rohrer. 1986. Atomic force microscopy. *Phys. Rev. Lett.* 56:930.

Celia, H., E. Wilson-Kubalek, R. A. Milligan, and L. Teyton. 1999. Structure and function of a membrane-bound murine MHC class I molecule. *Proc. Natl. Acad. Sci. USA.* 96:5634–5639.

Dammer, U., M. Hegner, D. Anselmetti, P. Wagner, M. Dreier, W. Huber, and H.-J. Güntherodt. 1995. Specific antigen/antibody interactions observed by the atomic force microscope. *Biophys. J.* 70:2437–2441.

Dietrich, C., O. Boscheinen, K.-D. Scharf, L. Schmitt, and R. Tampé. 1996. Functional immobilization of a DNA-binding protein at a membrane interface via histidine tag and synthetic chelator lipids. *Biochemistry.* 35:1100–1105.

Dietrich, C., L. Schmitt, and R. Tampé. 1995. Molecular organization of histidine-tagged biomolecules at self-assembled lipid interfaces using a novel class of chelator lipids. *Proc. Natl. Acad. Sci. USA.* 92: 9014–9018.

Dorn, I. T., R. Eschrich, E. Seemüller, R. Guckenberger, and R. Tampé. 1999. High-resolution AFM-imaging and mechanistic analysis of the 20S proteasome. *J. Mol. Biol.* 288:1027–1036.

Dorn, I. T., K. R. Neumaier, and R. Tampé. 1998. Molecular recognition of histidine tagged molecules by metal-chelating lipids monitored by fluorescence energy transfer and correlation spectroscopy. *J. Am. Chem. Soc.* 120:2753–2763.

Evans, E., and K. Ritchie. 1997. Dynamic strength of molecular adhesion bonds. *Biophys. J.* 72:1541–1555.

Florin, E.-L., V. T. Moy, and H. E. Gaub. 1994. Adhesive forces between individual ligand-receptor pairs. *Science.* 264:415–417.

Florin, E. L., M. Rief, H. Lehmann, M. Ludwig, C. Dornmaier, V. T. Moy, and H. E. Gaub. 1995. Sensing specific molecular interactions with the atomic force microscope. *Biosensors Bioelectron.* 10:895–901.

Gritsch, S., K. Neumaier, L. Schmitt, and R. Tampé. 1995. Engineered fusion molecules at chelator lipid interfaces imaged by reflection interference contrast microscopy (RICM). *Biosensors Bioelectron.* 10: 805–812.

Hochuli, E. 1990. Purification of recombinant proteins with metal chelate adsorbent. *Gen. Eng.* 12:87–98.

Hochuli, E., W. Bannwart, H. Döbeli, R. Gentz, and D. Stüber. 1988. Genetic approach to facilitate purification of recombinant proteins with a novel metal chelating adsorbent. *BioTechniques.* 1321–1325.

Ill, C. R., V. M. Keivens, J. E. Hale, K. K. Nakamura, R. A. Jue, S. Cheng, E. D. Melcher, B. Drake, and M. C. Smith. 1993. A COOH-terminal peptide confers regiospecific orientation and facilitates atomic force microscopy of an IgG1. *Biophys. J.* 64:919–924.

Kubalek, E. M., S. F. J. LeGrice, and P. O. Brown. 1994. Two-dimensional crystallization of histidine-tagged, HIV-1 reverse transcriptase promoted by a novel nickel-chelating lipid. *J. Struct. Biol.* 113:117–123.

Laibinis, P. E., J. J. Hickmann, M. S. Wrighton, and G. M. Whitesides. 1989. Orthogonal self-assembled monolayers: alkanethiols on gold and alkane carboxylic acids on alumina. *Science.* 245:845–847.

Lee, G. U., L. A. Chris, and R. J. Colton. 1994a. Direct measurements of the forces between complementary strands of DNA. *Science.* 266: 771–773.

Lee, G. U., D. A. Kidwell, and R. J. Colton. 1994b. Sensing discrete streptavidine-biotin interactions with the atomic force microscope. *Langmuir.* 10:354–357.

Löfås, S. 1995. Dextran modified self-assembled monolayer surfaces for use in biointeraction analysis with surface plasmon resonance. *Pure Appl. Chem.* 67:829–834.

Löfås, S., and B. Johnson. 1990. A novel hydrogel matrix on gold surfaces in surface plasmon resonance sensors for fast and efficient covalent immobilization of ligands. *J. Chem. Soc.* 1526–1528.

Ludwig, M., W. Dettmann, and H. E. Gaub. 1997. AFM imaging contrast based on molecular recognition. *Biophys. J.* 72:445–448.

Merkel, R., P. Nassoy, A. Leung, K. Ritchie, and E. Evans. 1999. Energy landscapes of receptor-ligand bonds explored with dynamic force spectroscopy. *Nature.* 397:50–53.

Moy, V. T., E.-L. Florin, and H. E. Gaub. 1994. Intermolecular forces and energies between ligands and receptors. *Science.* 266:257–259.

Pale-Grosdemange, C., E. S. Simon, K. L. Prime, and G. M. Whitesides. 1991. Formation of self-assembled monolayers by chemisorption of derivatives of oligo(ethylene glycol) of structure $HS(CH_2)_{11}(OCH_2CH_2)_mOH$ on gold. *J. Am. Chem. Soc.* 113:12–20.

Prime, K. L., and G. M. Whitesides. 1993. Adsorption of proteins onto surfaces containing end-attached oligo(ethylene oxide): a model system using self-assembled monolayers. *J. Am. Chem. Soc.* 115:10714–10721.

Rief, M., H. Clausen-Schaumann, and H. E. Gaub. 1999a. Sequence-dependent mechanics of single DNA molecules. *Nature Struct. Biol.* 6:346–349.

Rief, M., M. Gautel, M. Oesterhelt, J. M. Fernandez, and H. E. Gaub. 1997a. Reversible unfolding of individual titin immunoglobulin domains by AFM. *Science.* 276:1109–1112.

Rief, M., M. Gautel, A. Schimmel, and H. E. Gaub. 1998. The mechanical stability of immunoglobulin and fibronectin III domains in the muscle protein titin measured by atomic force microscopy. *Biophys. J.* 75: 3008–3016.

Rief, M., F. Oesterhelt, B. Heymann, and H. E. Gaub. 1997b. Single molecule spectroscopy on polysaccharides by atomic force microscopy. *Science.* 275:1295–1297.

Rief, M., J. Pascual, M. Saraste, and H. E. Gaub. 1999b. Single molecule force spectroscopy of spectrin repeats: low unfolding forces in helix bundles. *J. Mol. Biol.* 286:553–561.

Schmitt, L., T. M. Bohanon, S. Denzinger, H. Ringsdorf, and R. Tampé. 1996. Specific protein docking to chelator lipid monolayers monitored by FT-IR spectroscopy at the air-water interface. *Angew. Chem. Int. Ed. Engl.* 35:317–320.

Schmitt, L., C. Dietrich, and R. Tampé. 1994. Synthesis and characterization of chelator-lipids for reversible immobilization of engineered proteins at self-assembled lipid interfaces. *J. Am. Chem. Soc.* 116: 8485–8491.

Shnek, D. R., D. W. Pack, D. Y. Sasaki, and F. H. Arnold. 1994. Specific protein attachment to artificial membranes via coordination to lipid-bound copper(II). *Langmuir.* 10:2382–2388.

Sigal, G. B., C. Bandad, A. Barberis, J. Strominger, and G. M. Whitesides. 1996. A self-assembled monolayer for the binding and study of histidine-tagged proteins by surface plasmon resonance. *Anal. Chem.* 68: 490–497.

Simson, D. A., M. Strigl, M. Hohenadl, and R. Merkel. 1999. Statistical breakage of a single protein A-IgG bond reveals crossover from spontaneous to force-induced bond dissociation. *Phys. Rev. Lett.* 83: 652–655.

Venien-Bryan, C., F. Balavoine, B. Toussaint, C. Mioskowski, E. A. Hewat, B. Helme, and P. M. Vignais. 1997. Structural study of the response regulator HupR from *Rhodobacter capsulatus*. Electron microscopy of two-dimensional crystals on a nickel-chelating lipid. *J. Mol. Biol.* 274:687–692.

Wilson-Kubalek, E. M., R. E. Brown, H. Celia, and R. A. Milligan. 1998. Lipid nanotubes as substrates for helical crystallization of macromolecules. *Proc. Natl. Acad. Sci. USA.* 95:8040–8045.